
Precision Laser Spectroscopy of Li^+ and Neutral Lithium

W. A. van Wijngaarden, and G. A. Noble

Physics Department, York University, Toronto, ON, M3J 1P3, Canada
waww@yorku.ca

Abstract. Lithium has a number of properties that make it useful for both experimental and theoretical study. Precise spectroscopic measurements of optical transitions in both Li^+ and neutral Li are reviewed. Experiments have yielded hyperfine and fine structure splittings that test QED as well as isotope shifts that determine the relative nuclear charge radius between isotopes to an accuracy of 2×10^{-17} m. Experimental and theoretical results agree very well for Li^+ and a measurement of the fine structure of the $1s2p\ ^3P_{0,1,2}$ levels is of interest to determine the fine structure constant. For neutral lithium, additional theoretical work is needed to match the experimental accuracy for the $2P$ fine structure splitting.

1 Introduction

Lithium is the lightest naturally occurring solid element in the periodic table. It has a number of properties that make it a preferred atom to study for experimentalists including a relatively low melting point of 180°C that facilitates the generation of an atomic beam and most importantly for the application of precise spectroscopic techniques, transitions at visible wavelengths where continuous wave lasers readily operate. These transitions include the Li^+ $1s2s\ ^3S_1 \rightarrow 1s2p\ ^3P_{0,1,2}$ at 548 nm and the D lines in neutral lithium at 670 nm. Lithium has a number of isotopes, two of which are stable, as shown in Table 1. This is important when doing precise experiments where nuclear effects are comparable or exceed the measurement accuracy. The experiment can then be repeated using different isotopes whose nuclear size differ markedly. This is especially important for ^{11}Li which has been found to have halo neutrons [1].

Lithium is a multielectron system that precludes a simple analytic solution to the Schrödinger equation. Theoretical progress remained limited until about 15 years ago when G. W. F. Drake and collaborators began applying the so-called Hylleraas variational method to initially model two-electron and more recently three-electron systems [4]. Extensive computations using thousands of carefully constructed basis functions to represent the wavefunction have

Table 1. Lithium isotopes

Isotope	Natural Abundance	Nuclear Spin	Lifetime (msec)
${}^6\text{Li}$	7.5%	1	
${}^7\text{Li}$	92.5%	3/2	
${}^8\text{Li}$		2	836 ± 6 [2]
${}^9\text{Li}$		3/2	178.3 ± 0.4 [2]
${}^{11}\text{Li}$		3/2	8.59 ± 0.14 [3]

enabled the non-relativistic eigenenergies for helium states to be found with an accuracy of one part in 10^{16} [5]. These wavefunctions have in turn been used to perturbatively evaluate relativistic, hyperfine and QED terms to high accuracy. Comparison of theoretical energy estimates to measured isotope shifts has permitted the determination of the nuclear charge radius with an order of magnitude higher accuracy than is possible in electron scattering experiments [6, 7].

Several review articles give detailed descriptions of the various experimental techniques used to measure isotope shifts, fine and hyperfine splittings in neutral and singly ionized lithium [8, 9]. This article presents the results of the most accurate experiments and emphasizes recent work that has yielded improved values of the relative charge radii for the various lithium isotopes [6, 7, 10].

This paper is organized as follows. First, Sect. 2 gives a brief background of the theoretical and experimental techniques used in the most recent work. Next in Sect. 3, experimental data for the hyperfine and fine structure splittings found for the Li^+ $1s2s$ ${}^3\text{S}_1$ and $1s2p$ ${}^3\text{P}_{0,1,2}$ states are presented and compared to theory. The possibility of determining the fine structure constant from an improved measurement of the $1s2p$ ${}^3\text{P}_{0,1,2}$ fine structure splittings is examined. Section 4 presents results for the 2P fine structure as well as the D1 and D2 isotope shifts. The latter allow the determination of the relative nuclear charge radii of the various lithium isotopes. Finally, conclusions regarding the status of the work are made.

2 Background

The energy of an atom or ion having a nucleus with charge Z can be expressed as

$$E = E_{\text{NR}} + Z^2\alpha^2 E_{\text{Rel}} + Z^4\alpha^3 E_{\text{QED}} + E_{\text{Hyp}} + E_{\text{Nuc}} . \quad (1)$$

Here, E_{NR} is the sum of the kinetic energy of the electrons and the Coulomb interaction of the electrons with each other and with the nucleus. For light atoms such as lithium, E_{NR} is about 10^4 times larger than the relativistic

correction term $Z^2\alpha^2 E_{\text{Rel}}$ where α is the fine structure constant. E_{QED} represents the QED corrections whose largest term is the Lamb shift while E_{Hyp} is the hyperfine interaction. The finite size of the nucleus is described by [11]

$$E_{\text{Nuc}} = \frac{2\pi Z e^2 r_c^2}{3} \langle \Sigma_i \delta(\mathbf{r}_i) \rangle, \quad (2)$$

where r_c is the nuclear charge radius, e is the charge of the proton and the summation term equals the expectation value of the electron density at the nucleus where i is summed over all the electrons.

E_{Rel} , E_{QED} , E_{Hyp} and E_{Nuc} can be evaluated if highly accurate wavefunctions corresponding to the non-relativistic energy E_{NR} are known. These wavefunctions have been found using a so-called Hylleraas basis set [4]. The required computational time increases rapidly with the electron number. Hence, Li^+ is much easier to model than neutral lithium. Precisely measured hyperfine and fine structure intervals provide a stringent test of the theoretical calculations. The computed wavefunctions can also be used in conjunction with measured isotope shifts to determine the nuclear charge radius r_c .

A common technique to determine a frequency interval is to use a narrow linewidth laser to excite the transitions to the two energy levels. One then measures the absolute laser frequency to high accuracy for each transition. In practice, two separate lasers are commonly used. Each laser is locked to one of the transitions and the frequency difference of the two lasers is found by focussing part of each laser beam onto a fast photodiode and measuring the beat frequency [12]. Large frequency intervals can be found by locking one laser beam to an iodine reference transition [13]. Recently, the femtosecond frequency comb has simplified absolute frequency measurements [14]. However, accurately locking a laser to a line center may not be possible for transitions to various hyperfine levels and/or different isotopes that overlap. In that case, it is essential to examine the entire spectrum.

3 Li^+ $(1s)^2 \ ^3S \rightarrow 1s2p \ ^3P$ Transition

Our group has developed a method to measure frequency intervals whereby an electro-optically modulated laser beam excites either an ion (LIBEO) or neutral atomic beam (LABEO) that is illustrated in Fig. 1 [15, 16]. It requires only a single laser having frequency ν that is passed through either an acousto or electro-optic modulator (EOM). The modulation frequency is conveniently specified by a frequency synthesizer to one part in 10^7 . The output laser beam then has frequencies ν , $\nu \pm n\nu_{\text{mod}}$ where n is an integer. Fluorescence, generated by the radiative decay of the excited state, is detected by a photomultiplier (PMT) as the laser is scanned across the resonance. Each transition therefore generates multiple peaks in the spectrum that are separated by the modulation frequency which in turn permits calibration of the

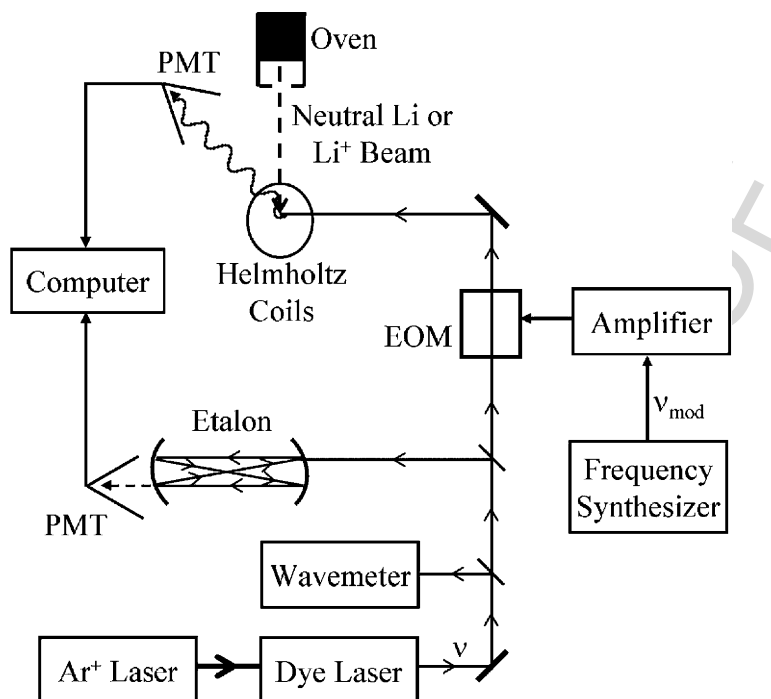


Fig. 1. Apparatus. See text for a description. For the case of a neutral atomic beam, Helmholtz coils surround the region where the laser and atomic beams intersect to cancel the Earth's magnetic field

frequency scan. The linearity of the laser scan is checked by monitoring the transmission of part of the laser beam through a Fabry–Perot etalon.

This technique was used to study the $\text{Li}^+ 1s2s \ ^3S_1 \rightarrow 1s2p \ ^3P_{0,1,2}$ transition [17]. The various hyperfine levels corresponding to this transition are shown in Fig. 2 for $^{6,7}\text{Li}^+$. The $\text{Li}^+ 1s2s \ ^3S_1$ state is 59 eV above the ground state and has a lifetime of 59 sec. It was produced by colliding an electron beam with a neutral Li beam. The ions were then passed through a Wien filter. A Faraday cup measured a Li^+ current of 250 nA. An argon ion laser pumped a ring dye laser that had a linewidth of 0.5 MHz. The dye laser beam was directed nearly collinearly to the ion beam. A wavemeter was used to coarsely tune the dye laser wavelength in order to locate the resonance. Fluorescence was detected by a liquid nitrogen cooled photomultiplier.

Figure 3 shows a sample signal obtained when a dye laser beam electro-optically modulated at 9.200000 GHz excited the transition. The peaks generated by the laser beam frequency shifted by ν_{mod} , have a smaller amplitude as most of the laser power was not frequency shifted. The fluorescent peaks have an asymmetric shape because of the non-Gaussian distribution of ion velocities. The etalon transmission peaks occurred nearly every 300 MHz

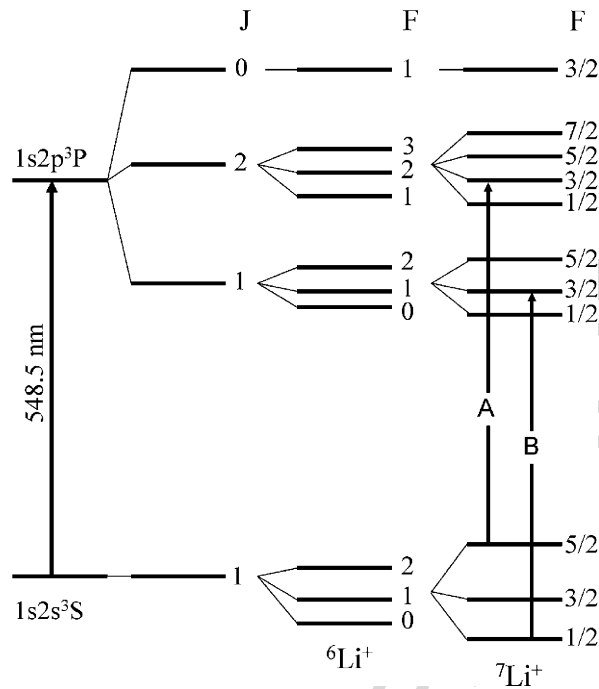


Fig. 2. Fine and hyperfine levels involved in the $\text{Li}^+ 1s2s \ ^3S_1 \rightarrow 1s2p \ ^3P_{0,1,2}$ transition. The vertical axis is not drawn to scale

corresponding to the free spectral range of the Fabry–Perot etalon. The free spectral range of the confocal etalon was monitored for each laser scan using the electro-optic modulation frequency to account for any change of the etalon length caused by temperature or pressure fluctuations. The laser scan was found to be linear to better than one part in 10^3 . The position of each fluorescence peak relative to the nearest Fabry–Perot peak was determined using a fifth-order polynomial to interpolate between the six nearest Fabry–Perot peak centers to account for any non-linearity of the laser frequency scan.

The measured hyperfine splittings are shown in Table 2. There is excellent agreement with the results for the $1s2s \ ^3S_1$ hyperfine splittings obtained by a so-called laser microwave (LM) experiment [18]. The latter method used a laser to excite the ions before they passed through a microwave region. The laser excitation depleted one hyperfine level of the metastable $1s2s \ ^3S_1$ state which was in turn repopulated if the microwaves were in resonance with a transition between the metastable state hyperfine levels. A second laser beam then probed the ions after the microwave region. The data from both experiments is in excellent agreement with the calculated values [12].

Our experiment determined the $1s2p \ ^3P_{1,2}$ fine structure splitting by measuring the frequency difference between transitions A and B shown in Fig. 2 and using the appropriate hyperfine splittings. Table 3 shows our result agrees

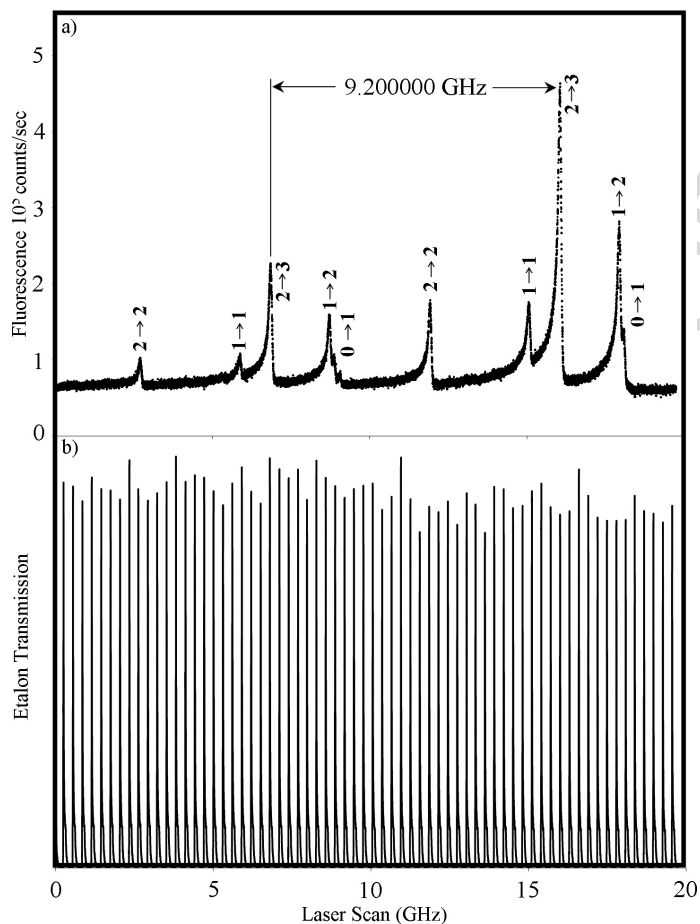


Fig. 3. (a) Fluorescent signal recorded as laser frequency modulated at 9.200000 GHz was scanned across Li^+ transitions labeled between hyperfine levels $F \rightarrow F'$. (b) Transmission of dye laser beam through etalon

very well with that found by Riis et al. [12] who precisely measured absolute laser frequencies for transitions to the various fine structure levels using a fast ion beam (LIB). Both of these experiments differ sharply with the result found by Rong et al. [13] who performed a laser heterodyne (LH) experiment using two frequency-locked dye lasers. One laser was locked to the Li^+ transition while the second laser was locked to an iodine transition. A portion of each laser beam was then focussed onto a fast photodiode that was connected to a frequency counter that measured the beat frequency. The results of Rong et al. also disagree with the Hylleraas variational calculation [12] for both the $1s2p \ ^3P_{1-2}$ and $\ ^3P_{0-1}$ fine structure intervals.

Table 2. Hyperfine splittings of ${}^6,7\text{Li}^+$ $1s2s\ {}^3\text{S}_1$ and $1s2p\ {}^3\text{P}_{1,2}$ states

Isotope	State	Interval	LIBEO [17] (MHz)	MW [18] (MHz)	Theory [12] (MHz)
${}^6\text{Li}$	$1s2s\ {}^3\text{S}_1$	2-1	6003.66 ± 0.51	6003.600 ± 0.050	6003.614 ± 0.024
		1-0	3001.83 ± 0.51	3001.780 ± 0.050	3001.765 ± 0.038
	$1s2p\ {}^3\text{P}_1$	2-1	2888.98 ± 0.59		2888.327 ± 0.029
		1-0	1316.06 ± 0.59		1317.649 ± 0.046
	$1s2p\ {}^3\text{P}_2$	3-2	4127.16 ± 0.76		4127.882 ± 0.043
		2-1	2857.00 ± 0.72		2858.002 ± 0.060
${}^7\text{Li}$	$1s2s\ {}^3\text{S}_1$	5/2-3/2	19817.90 ± 0.73	19817.673 ± 0.040	19817.680 ± 0.025
		3/2-1/2	11891.22 ± 0.60	11890.018 ± 0.040	11890.013 ± 0.038
	$1s2p\ {}^3\text{P}_1$	5/2-3/2	9966.30 ± 0.69	9965.2 ± 0.6	9966.14 ± 0.13
		3/2-1/2	4239.11 ± 0.54		4238.86 ± 0.20
	$1s2p\ {}^3\text{P}_2$	7/2-5/2	11774.04 ± 0.94	11775.8 ± 0.5	11773.05 ± 0.18
		5/2-3/2	9608.90 ± 0.49		9608.12 ± 0.15
		3/2-1/2	6204.52 ± 0.80	6203.6 ± 0.5	6203.27 ± 0.30

Table 3. $\text{Li}^+ 1s2p \ ^3\text{P}$ fine structure splittings

Interval	Experiment (MHz)	Technique	Theory[19] (MHz)
$^3\text{P}_{1-2}$	62667.4 ± 2.0	LH [13]	62679.4 ± 0.5
	62678.41 ± 0.65	LIB [12]	
	62679.46 ± 0.98	LIBEO [17]	
$^3\text{P}_{0-1}$	155709.0 ± 2	LH [13]	155703.4 ± 1.5
	155704.27 ± 0.66	LIB[12]	

Our experimental uncertainty arises from the asymmetric lineshape of the fluorescent peaks. The full width at half maximum (FWHM) natural linewidth estimated using the 44 ns radiative lifetime of the $1s2p \ ^3\text{P}$ state is 3.7 MHz. Hence, an experiment that determined the line center to 0.1% as is done in other careful spectroscopic work has the potential to determine the $1s2p \ ^3\text{P}_{0-1}$ interval to one part in 4×10^8 . Such an experiment could be done using a single ion in a trap or a so-called optical double resonance experiment [8]. It would be interesting if theory could calculate the fine structure to a few kHz as this would then enable the determination of the fine structure constant. Work is underway to evaluate higher order QED effects [19]. It would be of interest to compare such a result for α with the recent value as determined by the electron $g-2$ experiment [20, 21].

4 Li D Lines

The lithium D lines have been studied by a number of different experimental techniques [8, 22]. The advantage of our method using an electro-optically modulated laser to excite an atomic beam is that one single experiment yields information about the hyperfine intervals of both the ground and excited states, the 2P fine structure splitting as well as the D1 and D2 isotope shifts [10]. A stringent test is to check that the result for the ground state hyperfine splitting agrees with the value obtained using the atomic beam magnetic resonance method which is known to one part in 10^9 [23]. Our measured $2\text{S}_{1/2}$ hyperfine splittings are within 40 kHz of the accepted values for both ^6Li , ^7Li .

Figure 4 illustrates the 12 lines comprising the D lines. The experiment used a neutral atomic beam of lithium that was orthogonally intersected by a laser beam to eliminate the first-order Doppler shift. Electro-optic modulators operating at 6.8 and 9.2 GHz were used to avoid overlapping peaks. Data were taken separately using ^6Li and natural lithium as shown in Figs. 5 and 6, respectively. Data were recorded by a fast digital storage oscilloscope such that each point corresponded to a frequency interval of 12 kHz. The fluorescence peak positions were found by fitting a sum of Lorentzian functions to the

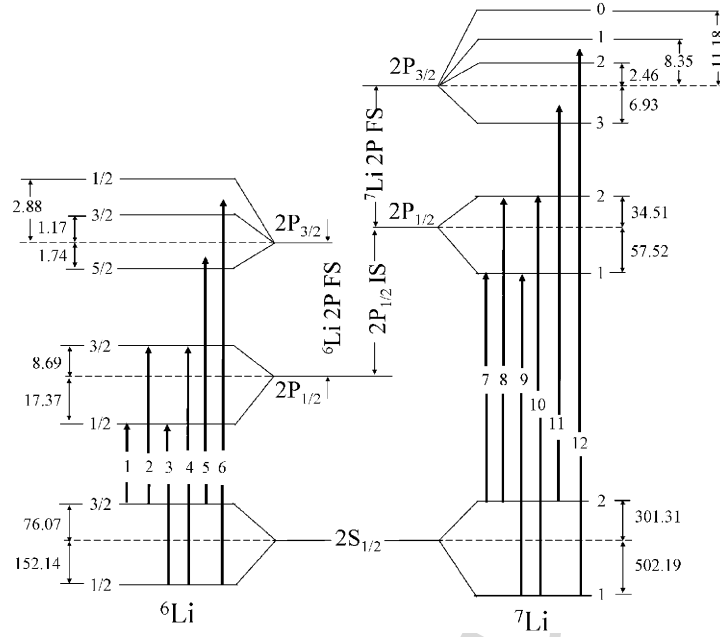


Fig. 4. Neutral lithium energy levels involved in D line transitions. The vertical energy axis is not drawn to scale. The positions of the various hyperfine levels are indicated relative to the center of gravity energy of a state $E_{\text{cg}} = \Sigma_F(2F + 1)E_F / \Sigma_F(2F + 1)$. All units are in MHz

spectrum using MATLAB 7.0. Each fluorescence peak position was found using the same procedure as described previously for the Li^+ work.

A complication arises in analyzing peaks 11 and 12 because the 5.8 MHz fullwidth at half maximum (FWHM) natural linewidth of the $2S$ - $2P$ transition is comparable to the ${}^7\text{Li}$ $2P_{3/2}$ hyperfine splittings as shown in Fig. 4. This causes the observed peaks to have an asymmetric shape as shown in Figs. 7 and 8. Peaks 11 and 12 were fit using three Lorentzian functions. The relative center frequencies of the three peaks were set equal to the $2P_{3/2}$ hyperfine intervals that were previously determined [24]. The red fitted curve appearing in each of Figs. 7 and 8 was found by varying the center frequency of the first peak appearing in the laser scan as well the amplitudes and widths of all three Lorentzian functions to obtain the optimum fit to the data.

For peak 11, the fluorescence is dominated by the radiative decay of the $F = 3$ hyperfine level of the $2P_{3/2}$ state. The linearly polarized laser beam preferentially excites more atoms from the $2S_{1/2}$ $F = 2$ level to the $F = 3$ level than to the $F = 2$ and $F = 1$ levels of the $2P_{3/2}$ state. Moreover, selection rules only allow the $2P_{3/2}$ $F = 3$ level to radiatively decay to the $F = 2$ ground state level from which it can be re-excited by the laser. In contrast,

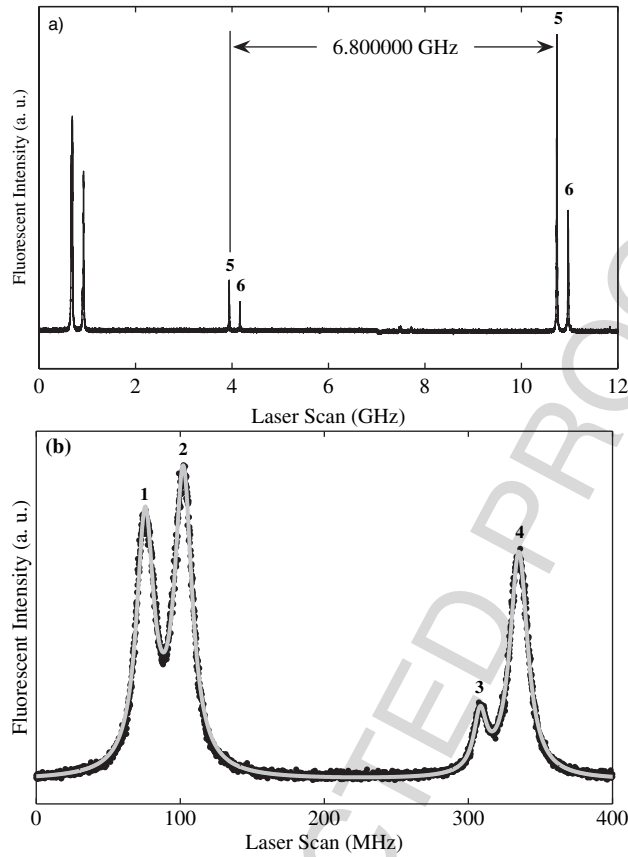


Fig. 5. Excitation of ${}^6\text{Li}$. (a) shows a scan where the laser-excited transitions 1–6 illustrated are in Fig. 4. The first four peaks are shown in (b) along with the red curve fitted to the data as is discussed in the text

the $2P_{3/2}$ $F = 1$ and 2 levels can also decay to the $F = 1$ ground state level which is not in resonance with the laser beam.

For peak 12, no one $2P_{3/2}$ hyperfine level has a dominant contribution to the fluorescent signal. This can be understood by modeling the effect of repeated excitation and radiative decay as an atom passes through the linearly polarized laser beam. An atom, initially entering the laser beam, was assumed to have all of its ground state hyperfine sublevels equally populated. A computer program modeled changes of the sublevel populations caused by the repeated laser excitation and radiative decay. The fluorescence contributions to peak 12 from the $2P_{3/2}$ $F = 0, 1$ and 2 hyperfine levels were predicted to be 28%, 36% and 36%, respectively. This compares very closely with the averaged fitted peak amplitude values of 29%, 34% and 37%.

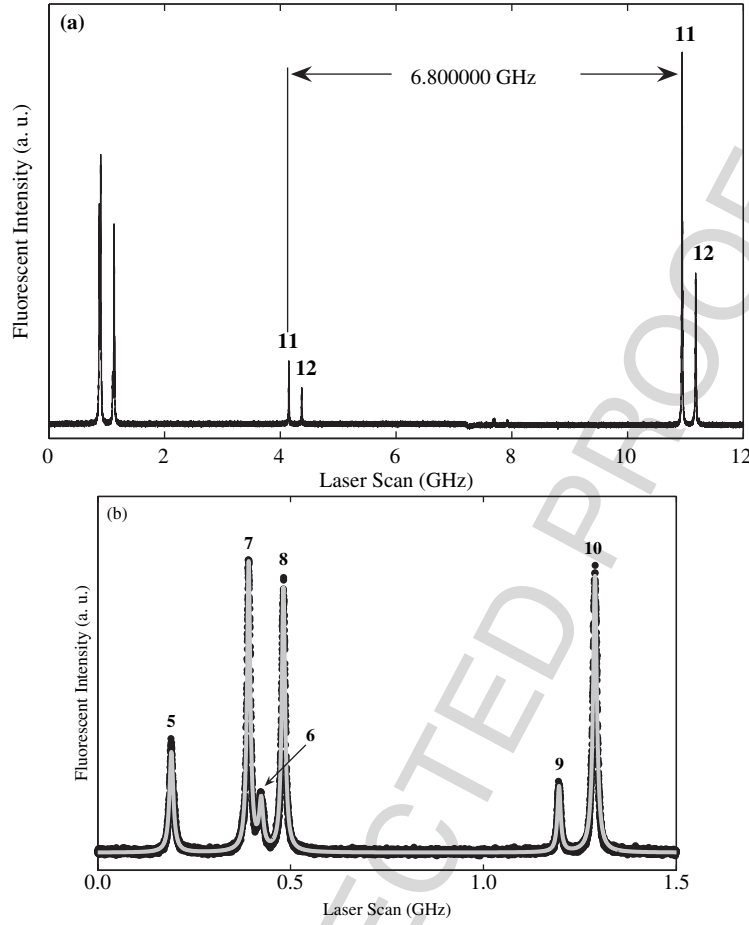


Fig. 6. Excitation of natural lithium. (a) shows a scan where transitions 5 and 6 of ^6Li and transitions 7–12 of ^7Li , as illustrated in Fig. 4, were excited. (b) shows the first six peaks where the red curve is fitted to the data as is discussed in the text

The 2P fine structure splittings were found by measuring the frequency difference between the D2 and D1 transitions illustrated in Fig. 4. For ^7Li , the 2P fine structure splitting was found by determining the frequency separating peaks 11 and 12 from peaks 7 to 10 and using the appropriate hyperfine splittings. Our hyperfine splittings of the $2P_{1/2}$ state agreed with the most accurate measurements in the literature [22]. The 2P fine structure splittings using peaks 11 and 12 were found to be 10053.116 ± 0.079 and 10053.123 ± 0.086 MHz, respectively. These two values were averaged to give the result listed in Table 4.

The ^6Li 2P fine structure was found as follows. The repeated excitation of the $2S_{1/2} F = 1/2$ level to the $2P_{3/2} F = 1/2$ and $3/2$ levels and their

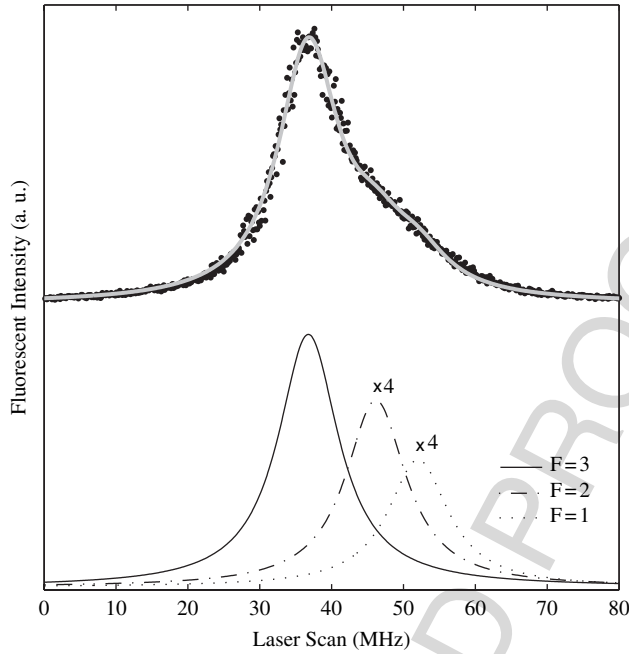


Fig. 7. Analysis of peak 11. The red fitted curve is comprised of three peaks to the $2P_{3/2}$ state hyperfine levels $F = 1, 2, 3$ as discussed in the text. The fluorescence contributions from the $2P_{3/2}$ $F = 1, 2$ hyperfine levels are magnified by a factor of 4

subsequent radiative decay do not affect the relative populations of the $2S_{1/2}$ $F = 1/2$ $m_F = \pm 1/2$ hyperfine sublevels. The fluorescence contributions from the $2P_{3/2}$ $F = 1/2$ and $3/2$ levels were calculated to be 47.8% and 52.2%, respectively. Hence, using the $2P_{3/2}$ hyperfine splitting, peak 6 is shifted 1.987 MHz above the $2P_{3/2}$ center of gravity as indicated in Fig. 4. The shift of peak 5 below the $2P_{3/2}$ center of gravity is found by measuring the frequency interval separating peaks 5 and 6 and subtracting the aforementioned shift of peak 6 and the hyperfine splitting of the ${}^6\text{Li}$ ground state which is known to very high accuracy [23]. The shifts of peaks 5 and 6 relative to the $2P_{3/2}$ center of gravity were comparable in magnitude but opposite in sign. Hence, the effect of these shifts was minimized by determining the ${}^6\text{Li}$ 2P fine structure by averaging the values obtained using peaks 5 and 6 relative to peaks 1–4 giving the result listed in Table 4.

The D1 isotope shift can be found by measuring the frequency intervals separating the ${}^6\text{Li}$ D1 transition peaks 1–4 from the corresponding ${}^7\text{Li}$ D1 peaks 7–10 and using the hyperfine splittings of the $2S_{1/2}$ and $2P_{1/2}$ states. Ideally, data would be taken using a lithium sample consisting of equal amounts of the two isotopes ${}^6,7\text{Li}$. This was not done as increasing the amount of ${}^6\text{Li}$ enhances the amplitude of peak 6 which overlaps with peaks 7 and 8.

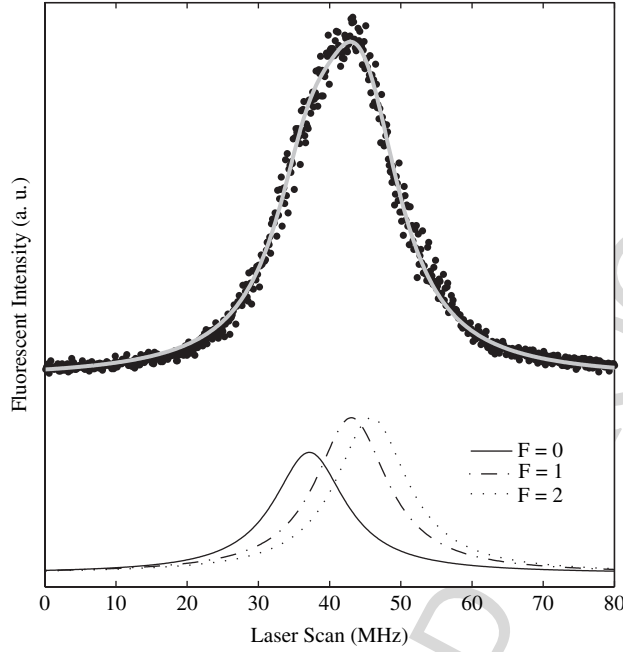


Fig. 8. Analysis of peak 12. The red fitted curve is comprised of three peaks to the $2P_{3/2}$ state hyperfine levels indicated as discussed in the text

The isotope shift was therefore found by first finding the separation of peaks 7–10 relative to peak 5 for scans obtained using natural lithium as shown in Fig. 6. The frequency interval separating peak 5 from peaks 1 to 4 was then found from laser scans using ^6Li as shown in Fig. 5.

Table 4. Neutral lithium 2P fine structure (FS) and D1 isotope shift

Quantity	Experiment (MHz)	Technique	Theory[25] (MHz)
^6Li 2P FS	10052.76 ± 0.22	LC [26]	10050.846 ± 0.012
	10051.62 ± 0.20	LAB[27]	
	10052.964 ± 0.050	LABEO[10]	
^7Li 2P FS	10053.24 ± 0.22	LC [26]	10051.214 ± 0.012
	10053.184 ± 0.058	ODR [28]	
	10053.4 ± 0.2	LAB [27]	
	10053.119 ± 0.058	LABEO [10]	
D1 Isotope Shift	10534.3 ± 0.3	LAB[29]	10534.12 ± 0.07
	10533.13 ± 0.15	LAB [27]	
	10533.160 ± 0.068	LAB [30]	
	10534.039 ± 0.070	LABEO[10]	

Table 4 lists the most accurate published 2P fine structure splittings. Our measurements agree very well with the results of level crossing spectroscopy (LC) [26] as well as an optical double resonance experiment (ODR) [28] for both ${}^6,{}^7\text{Li}$. There is only disagreement with the result for the ${}^6\text{Li}$ 2P fine structure interval as found by a laser atomic beam (LAB) measurement [27]. The latter experiment uses a Fabry–Perot etalon to monitor the change of the laser frequency during a scan. Unfortunately, it is difficult to maintain proper calibration of the etalon as its length can be affected by pressure and temperature fluctuations that have caused errors in previous work [31]. All of the experiments obtain values for the fine structure that are several MHz greater than the theoretical value [25]. The uncertainty listed for the theoretical value in Table 4 is the computational uncertainty. It does not consider the effect of QED correction terms proportional to α^4 times the Rydberg energy which for helium contribute several MHz to the fine structure splitting [32].

Table 4 also lists the most accurate published results for the D1 isotope shifts. Our value agrees with an earlier laser atomic beam measurement [29] and also is very close to the theoretical estimate [25] but disagrees with the two other measurements. Further insight into these isotope shifts can be obtained by determining the nuclear charge radius using [4]

$$\Delta r_c^2 = r_c^2({}^6\text{Li}) - r_c^2({}^7\text{Li}) = (\delta\nu_{jk} - \delta E_{jk})/C_{jk}. \quad (3)$$

Here, $\delta\nu_{jk}$ is the measured isotope shift for the transition between states j and k , δE_{jk} is the calculated isotope shift difference for the two states excluding the nuclear size correction E_{Nuc} and C_{jk} is proportional to the square of the electron wavefunction at the nucleus.

Table 5 lists the results for a number of experiments that studied various transitions in Li^+ and neutral Li. The data listed for the ${}^6\text{Li}$ nuclear charge radius r_c were found using the measured value for ${}^7\text{Li}$ of 2.39 ± 0.03 fm obtained in an electron scattering experiment [33]. Our result for the D2 isotope shift listed in Table 5 was obtained by adding the ${}^7\text{Li}$ 2P fine structure splitting to the D1 isotope shift and subtracting the ${}^6\text{Li}$ 2P fine structure splitting. An important test of each experiment is to check whether the results obtained for different transitions give consistent results. All three results for the Li^+ transitions made by Riis et al. [12] agree well with each other as do our results [10]. The two results for Δr_c^2 found by Scherf et al. [27] disagree by nearly 10 times the stated uncertainty. The remaining isotope shifts found for the Li $2\text{S}_{1/2} \rightarrow 3\text{S}_{1/2}$ transition and one value for the D1 isotope shift were all found by the same group. For the two photon $2\text{S}_{1/2} \rightarrow 3\text{S}_{1/2}$ transition, the atoms passed through an optical cavity that enhanced the power of the dye laser tuned at 610 nm. The uncertainty of their first measurement [30] apparently did not adequately take into account the ac Stark shift which was estimated in their later experiment to increase the uncertainty by 110 kHz [6, 7]. Both isotope shifts of their initial experiment yield results for Δr_c^2 which are lower than the results of our work, Riis et al. and an electron scattering experiment [33] as well as the results predicted by the nuclear theory [34].

Table 5. Determination of ${}^6\text{Li}$ nuclear charge radius. The measured isotope shifts are given by δE_{jk} , while δE_{jk} and C_{jk} were obtained by a Hylleraas variational calculation given in [4]. The first and second error bars in the columns for Δr_c^2 and r_c (${}^6\text{Li}$) are the total and experimental (bracketed) uncertainties

Transition	ν_{jk} (MHz)	δE_{jk} (MHz)	C_{jk}	Δr_c^2 (fm ²)	r_c (${}^6\text{Li}$) (fm)
$\text{Li}^+ (2\ ^3\text{S}_1 - 2\ ^3\text{P}_0)$	34747.73 ± 0.55 [12]	34740.17 ± 0.03	9.705	0.779 ± 0.057(0.057)	2.548 ± 0.031(0.011)
$\text{Li}^+ (2\ ^3\text{S}_1 - 2\ ^3\text{P}_1)$	34747.46 ± 0.67 [12]	34739.87 ± 0.03		0.782 ± 0.069(0.069)	2.548 ± 0.032(0.014)
$\text{Li}^+ (2\ ^3\text{S}_1 - 2\ ^3\text{P}_2)$	34748.91 ± 0.62 [12]	34742.71 ± 0.03		0.639 ± 0.064(0.064)	2.520 ± 0.031(0.031)
$\text{Li} (2\ ^2\text{S}_{1/2} - 3\ ^2\text{S}_{1/2})$	11453.95 ± 0.13 [7]	11453.01 ± 0.06	1.566	0.600 ± 0.091(0.083)	2.512 ± 0.033(0.018)
	11453.734 ± 0.030 [30]			0.462 ± 0.042(0.019)	2.485 ± 0.030(0.009)
$\text{Li} (2\ ^2\text{S}_{1/2} - 2\ ^2\text{P}_{1/2})$	10533.160 ± 0.068 [30]	10532.17 ± 0.07	2.457	0.403 ± 0.040(0.028)	2.473 ± 0.030(0.008)
	10533.13 ± 0.15 [27]			0.391 ± 0.067(0.061)	2.470 ± 0.032(0.014)
	10534.039 ± 0.070 [10]			0.761 ± 0.040(0.028)	2.544 ± 0.030(0.006)
$\text{Li} (2\ ^2\text{S}_{1/2} - 2\ ^2\text{P}_{3/2})$	10534.93 ± 0.15 [27]	10532.57 ± 0.07	2.457	0.961 ± 0.067(0.061)	2.592 ± 0.032(0.014)
	10534.194 ± 0.104 [10]			0.661 ± 0.050(0.042)	2.524 ± 0.030(0.009)
e-nuclear scattering [33]				0.842	2.56 ± 0.05
Nuclear theory [34]				0.740	2.54 ± 0.01

The value of Δr_c^2 obtained by averaging the results of the Riis experiment [12] that studied the $\text{Li}^+ 2^3\text{S}_1 \rightarrow 3^3\text{P}_{0,1,2}$ transitions and the Ewald experiment [6] that examined the $\text{Li } 2^3\text{S}_{1/2} \rightarrow 3^2\text{S}_{1/2}$ transition is 0.700 fm^2 . This is in excellent agreement with the average value of our two measured values of 0.704 fm^2 . However, the uncertainty of our results is due about equally to experimental and theoretical uncertainties whereas it is dominated by experimental effects in the other experiments. The uncertainties listed in Table 5 for $r_c(^6\text{Li})$ are dominated by the accuracy of $r_c(^7\text{Li})$. The average value of the ^6Li charge radius obtained by averaging the results of the experiments by Riis et al., Ewald et al. and our work is 2.53 fm which is listed in Table 6.

The charge radii of the radioactive lithium isotopes were found using the accelerator at the GSI facility in Darmstadt, Germany [6, 7]. The $^8,^9\text{Li}$ nuclei were generated using a 11.4 MeV/u beam of ^{12}C incident on a tungsten target. The reaction products were then ionized and passed through a magnetic mass separator before being stopped by a graphite foil. The graphite was heated to $1800 - 1900^\circ\text{C}$ using a 4 W CO_2 laser to enable the lithium to diffuse out of the foil. The lithium atoms were then laser ionized and detected after passing through a quadrupole mass spectrometer. $^8,^9\text{Li}$ beams of 2×10^5 and 1×10^5 atoms/sec were obtained. The atoms were laser ionized when they passed through an optical cavity. For the case of the two-photon $2\text{S}_{1/2} \rightarrow 3\text{S}_{1/2}$ transition, a dye laser operating at 610 nm was tuned to maximize the production of Li^+ . Part of this laser was focussed onto a fast photodiode along with a diode laser locked to an iodine reference line. The isotope shift was then found by measuring the beat frequency.

Table 6. Lithium charge and mass radii

Isotope	Δr_c^2 (fm) ²	Charge Radius (fm)	Mass Radius [1] (fm)
^6Li	0.636 ± 0.051	2.53 ± 0.03	2.35 ± 0.03
^7Li		2.39 ± 0.03 [33]	2.35 ± 0.03
^8Li	-0.43 ± 0.11	2.30 ± 0.04 [7]	2.38 ± 0.02
^9Li	-0.72 ± 0.14	2.24 ± 0.04 [7]	2.32 ± 0.02
^{11}Li			3.10 ± 0.17

Table 6 lists values for the charge and mass radii for the lithium isotopes. It is not surprising that the mass and charge radii differ as the quark constituents of the nuclei do not have equal charge. The mass radii of the radioactive lithium isotopes was determined by scattering an accelerator-generated beam of these nuclei from a target nucleus and measuring the interaction cross-section given by [1]:

$$\sigma_{\text{I}} = \pi[R_{\text{I}}^2 + R_{\text{T}}^2] . \quad (4)$$

Various targets composed of Be, C and Al were used in order to separately determine the radii of the target R_T and incoming nuclei R_I . The root mean square mass radius of the nucleon distribution was then deduced from R_I using a variety of nuclear models. Values for the mass radii found using the so-called Gaussian and harmonic oscillator nucleon distributions differed by less than the experimental uncertainties [35, 36]. The mass radius remains nearly constant for ${}^{6,7,8,9}\text{Li}$ while a small decrease is evident for the charge radius. It will be interesting to compare the mass and charge radii of ${}^{11}\text{Li}$ to determine whether the charge radius is also significantly perturbed by the halo neutrons as is the mass radius [37].

5 Conclusions

Important advances in both theory and experiment have been made in recent years in both Li^+ and neutral lithium. For the case of Li^+ it will be interesting to improve both the theory and measurement to reduce the uncertainty of the $1s2p\ 2\ ^3\text{P}$ fine and hyperfine structure splittings to 1 kHz. Future experiments with this level of accuracy would not only test QED but also enable the fine structure constant α to be determined with an accuracy competitive with other techniques that yield conflicting results [20, 21]. For the case of the neutral lithium D lines, the 2P fine structure as measured using a variety of techniques by a number of experimental groups, all agree. The theoretical result is significantly lower than the measured value. It is interesting that the variational calculations yield a D1 isotope shift that agrees much better with the experimental value than is the case with the fine structure. The reason is that various QED terms are mass independent and cancel in the calculation of an isotope shift but cannot be neglected when evaluating the fine structure [4]. Hence, further theoretical work to improve the estimate of the lithium 2P fine structure is needed.

Optically measured isotope shifts have permitted the nuclear charge radii of the various lithium isotopes to be found with an experimental uncertainty of ≤ 0.02 fm. It is remarkable that these experiments yield more accurate results than is obtained using electron scattering. Ironically, one now has a better understanding of how an electron in the lithium atom interacts with the nucleus than of how a macroscopic electron beam scatters from a Li nucleus. This underscores the incredible advances made in both atomic theory and experiment and motivates future work in both Li^+ and neutral lithium.

Acknowledgment

The authors would like to thank the Natural Science and Engineering Research Council of Canada for financial support.

References

1. I. Tanihata, T. Kobayashi, O. Yamakawa, S. Shimoura, K. Ekuni, K. Sugimoto, N. Takahashi, T. Shimoda and H. Sato: *Phys. Lett. B* **206**, 592 (1988).
2. Handbook of Chemistry and Physics 69th Edition, edited by R. C. Weast, (CRC Press, Boca Raton, 1988).
3. F. Schmitt, A. Dax, R. Kirchner, H. J. Kluge, T. Kühn, I. Tanihata, M. Wakasugi, H. Wang and C. Zimmermann: *Hyp. Inter.* **127**, 111 (2000).
4. G. W. F. Drake, W. Nörtershäuser and Z. C. Yan: *Can. J. Phys.* **83**, 311 (2005).
5. G. W. F. Drake: *Atomic, Molecular and Optical Physics Handbook*, edited by G. W. F. Drake (AIP, New York, 1996).
6. G. Ewald, W. Nörtershäuser, A. Dax, S. Götze, R. Kirchner, H. J. Kluge, T. Kühn, R. Sanchez, A. Wojtaszek, B. A. Bushaw, G. W. F. Drake, Z. C. Yan and C. Zimmerman: *Phys. Rev. Lett.* **93**, 113002 (2004).
7. G. Ewald, W. Nörtershäuser, A. Dax, S. Götze, R. Kirchner, H. J. Kluge, T. Kühn, R. Sanchez, A. Wojtaszek, B. A. Bushaw, G. W. F. Drake, Z. C. Yan and C. Zimmerman: *Phys. Rev. Lett.* **94**, 039901 (2005).
8. W. A. van Wijngaarden: *Can. J. Phys.* **83**, 327 (2005).
9. J. J. Clarke and W. A. van Wijngaarden: *Recent Res. Dev. Phys.* **3**, 347 (2002).
10. G. A. Noble, B. E. Schultz, H. Ming and W. A. van Wijngaarden: *Phys. Rev. A* **74**, 012502 (2006).
11. J. D. Morgan II and J. S. Cohen: *Atomic, Molecular and Optical Physics Handbook*, edited by G. W. F. Drake (AIP, New York, 1996).
12. E. Riis, A. G. Sinclair, O. Poulsen, G. W. F. Drake, W. R. C. Rowley and A. P. Levick: *Phys. Rev. A* **49**, 207 (1994).
13. H. Rong, S. Grafström, J. Kowalski, G. zu Putlitz, W. Jastrzebski and R. Neumann: *Z. Phys. D* **25**, 337 (1993).
14. T. Udem, J. Reichert, R. Holzwarth and T. W. Hänsch: *Opt. Lett.* **24**, 881 (1999).
15. W. A. van Wijngaarden: *Adv., At., Mol., Opt. Phys.* **36**, 141 (1996).
16. W. A. van Wijngaarden: *Proc. of Int. Conf. on Atomic Phys.* **16**, 305 (1999).
17. J. J. Clarke and W. A. van Wijngaarden: *Phys. Rev. A* **67**, 012506 (2003).
18. J. Kowalski, R. Neumann, S. Noehte, K. Scheffzek, H. Suhr and G. zu Putlitz: *Hyp. Int.* **15/16**, 15 (1983).
19. T. Zhang, Z. C. Yan and G. W. F. Drake: *Phys. Rev. Lett.* **77**, 1715 (1996).
20. G. Gabrielse, D. Hanneke, T. Kinoshita, M. Nio and B. Odom: *Phys. Rev. Lett.* **97**, 030802 (2006).
21. G. W. F. Drake: *Can. J. Phys.* **80**, 1195 (2002).
22. J. Walls, R. Ashby, J. J. Clarke, B. Lu and W. A. van Wijngaarden: *Eur. Phys. J. D* **22**, 159 (2003).
23. A. Beckmann, K. D. Böklen and D. Elke: *Z. Phys.* **270**, 173 (1974).
24. E. Arimondo, M. Inguscio and P. Violino: *Rev. Mod. Phys.* **49**, 31 (1977).
25. Z. C. Yan and G. W. F. Drake: *Phys. Rev. A* **66**, 042504 (2002).
26. K. C. Brog, T. G. Eck and H. Wieder: *Phys. Rev.* **153**, 91 (1967).
27. W. Scherf, O. Khait, H. Jäger and L. Windholz: *Z. Phys. D: At. and Mol. Clusters* **36**, 31 (1996).
28. H. Orth, H. Ackermann and E. W. Otten: *Z. Phys. A* **273**, 221 (1975).
29. L. Windholz, H. Jäger, M. Musso and G. Zerza: *Z. Phys. D: At., Mol. Clusters* **16**, 41 (1990).

30. B. A. Bushaw, W. Nörtershäuser, G. Ewald, A. Dax and G. W. F. Drake: *Phys. Rev. Lett.* **91**, 043004 (2003).
31. C. Umfer, L. Windholz and M. Musso: *Z. Phys. D: At., Mol. Clusters* **25**, 23 (1992).
32. G. W. F. Drake, I. B. Khriplovich, A. I. Milstein and A. S. Yelkhovsky: *Phys. Rev. A* **48**, R15 (1993).
33. C. W. de Jager, H. de Vries and C. de Vries: *At. Nucl. Data Tables* **36**, 495 (1987).
34. S. C. Pieper, V. R. Pandharipande, R. B. Wiringa and J. Carlson: *Phys. Rev. C* **64**, 014001 (2001).
35. I. Tanihata, H. Hamagaki, O. Hashimoto, Y. Shida, N. Yoshikawa, K. Sugimoto, O. Yamakawa, T. Kobayashi and N. Takahashi: *Phys. Rev. Lett.* **55**, 2676 (1985).
36. R. B. Elton: *Nuclear Sizes* (Oxford Univ. Press, Oxford, 1961).
37. W. Nörtershäuser, A. Dax, G. Ewald, I. Katayama, R. Kirchner, H. J. Kluge, T. Kühl, R. Sanchez, I. Tanihata, M. Tomaselli, H. Wang and C. Zimmermann: *Nucl. Instr. and Methods in Phys. Res. B* **204** 644 (2003).

UNCORRECTED PROOF